

# Year 1 Report: Evaluation and Improvement of Ocean Model Parameterizations for NCEP Operations

**PI: Dr. Lynn K. Shay**  
**Co-PI: George Halliwell**  
**NCEP Collaborator: Dr. Carlos Lozano**

RSMAS/MPO, University of Miami – 4600 Rickenbacker Causeway, Miami, FL 33149, USA  
Phone: (305) 421-4075 - Fax: (305) 421-4696 - Email: [nick@rsmas.miami.edu](mailto:nick@rsmas.miami.edu) –  
Internet: <http://isotherm.rsmas.miami.edu/~nick>

---

**Goal:** The long term goal of this NOAA Joint Hurricane Testbed (JHT) grant is to evaluate and improve ocean model parameterizations in NOAA National Centers for Environmental Prediction (NCEP) coupled hurricane forecast models in collaboration with the NOAA Tropical Prediction Center (TPC) and NOAA/NCEP Environmental Modeling Center (EMC). This effort targets the Joint Hurricane Testbed programmatic priorities **EMC-1** and **EMC-2** along with hurricane forecaster priorities **TPC-1** and **TPC-2** that focus on improving intensity forecasts through evaluating and improving oceanic boundary layer performance in the coupled model and improving observations required for model initialization, evaluation, and analysis. This project will be conducted under the auspices of the Cooperative Institute of Marine and Atmospheric Science program, and addresses **CIMAS Theme 5: Air-Sea Interactions and Exchanges** and **NOAA Strategic Goal 3: Weather and Water (local forecasts and warnings)**.

Specific objectives of this grant are:

- i) optimizing spatial resolution that will permit the ocean model to run efficiently as possible without degrading the simulated response;
- ii) improving the initial background state provided to the ocean model;
- iii) improving the representation of vertical and horizontal friction and mixing;
- iv) generating the realistic high-resolution atmospheric forcing fields necessary to achieve the previous objectives; and
- v) interacting with NOAA/NCEP/EMC in implementing ocean model code and evaluating the ocean model response in coupled hurricane forecast tests

**Progress:** This effort has proceeded along two closely related tracks: the preparation and analysis of the *in-situ* ocean observations required to evaluate ocean model performance, and the thorough evaluation of ocean model performance using these and other available ocean observations. The observational effort includes processing in situ Acoustic Doppler Current Profiler (ADCP) data from Ivan (provided by the U.S. Naval Research Laboratory), moored observations during Katrina and Rita (data courtesy of Minerals Management Service-MMS), and NOAA Hurricane Research Division (HRD) Intensity Fluctuation Experiments (IFEX) observations for pre and post Rita in 2005 (Rogers *et al.*, 2006; Jaimes and Shay, 2009, 2010). In addition, oceanic and atmospheric profiler measurements were acquired during hurricanes Gustav and Ike in 2008 in and over the Gulf of Mexico. In all these cases, satellite observations (altimetry and SST) have been obtained and Ocean Heat Content (OHC) maps have been produced following the Shay and Brewster (2010) approach.

The centerpiece of the modeling effort to date has been a thorough evaluation of ocean model performance during Hurricane Ivan (2004) designed to address the specific objectives listed above. A paper describing these results including detailed comparisons to oceanic observations (Halliwell *et al.*, 2010) is in press in *Monthly Weather Review*. Reference experiments have also been performed for Hurricanes Katrina and Rita (05). These experiments have demonstrated that accurate ocean model initialization with respect to upper-ocean temperature and salinity (density) profiles along with the correct location of ocean currents and eddies is the most important factor influencing the accuracy of SST cooling forecast by an ocean model. Efforts are now underway to evaluate existing ocean model initialization products prior to a large number of storms to quantify errors and biases and to design observational strategies to improve the initial ocean fields.

Table 1. Summary of the 15 numerical experiments simulating the ocean response to hurricane Ivan conducted in the GOM domain. Key model attributes that are varied are broken into major categories and listed in column 1. Characteristics of the control experiment are listed in column 2 while the single model attributes varied in each of the remaining experiments are listed in column 3.

Model Attribute	Control Experiment (GOM1)	Alternate Experiments
Horizontal resolution	0.04° Mercator	<b>GOM2:</b> 0.08° Mercator
Vertical resolution	26 layers, 4-8m in OML	<b>GOM3:</b> 21 layers, 7.5-15m in OML <b>GOM4:</b> 31 layers, 3-5m in OML
Vertical mixing	KPP	<b>GOM5:</b> MY <b>GOM6:</b> GISS
$C_D$	Donelan	<b>GOM7:</b> Powell <b>GOM8:</b> Large and Pond <b>GOM9:</b> Large and Pond (capped) <b>GOM10:</b> Shay and Jacob <b>GOM11:</b> Jarosz <i>et al.</i>
$C_{EL}$ , $C_{ES}$	COARE3.0 algorithm	<b>GOM12:</b> Kara <i>et al.</i>
Atmospheric forcing	27-km COAMPS+H*WIND	<b>GOM13:</b> 27-km COAMPS only
Outer model	NCODA GOM hindcast	<b>GOM14:</b> Free GOM simulation
Ocean dynamics	Three-dimensional	<b>GOM15:</b> One-dimensional

**Modeling:** The Hybrid Coordinate Ocean Model (HYCOM) is the chosen ocean model because it is being evaluated as the ocean model component of the next-generation coupled hurricane forecast model under development at NOAA/NCEP/EMC. It also contains multiple choices of numerical schemes and subgrid-scale parameterizations, making it possible to isolate model sensitivity to individual processes and devise strategies to improve model representation of these processes. In this context, fifteen free-running HYCOM simulations were conducted to assess model sensitivity to vertical resolution in the surface mixed layer, horizontal resolution, vertical mixing scheme, wind stress drag coefficient, surface turbulent flux drag coefficient, resolution of surface forcing, accuracy of ocean model initialization, and ocean dynamics (one dimensional versus three dimensional) for hurricane Ivan (numerical experiments are listed in Table 1). All experiments were conducted within a GOM domain where the coastline follows the actual land/sea boundary with a minimum water depth of 2 m. They are all nested within an outer model and are forced by surface fields of vector wind stress, wind speed, surface atmospheric

temperature and humidity, longwave and shortwave radiation, and precipitation. Surface turbulent heat fluxes and evaporation are calculated during model runs using bulk formula. Freshwater input from 12 rivers is included.

A control experiment (GOM1) is performed that is forced by atmospheric fields from the 27 km resolution COAMPS model of the U. S. Navy, but with high-resolution wind speed and stress fields obtained from the NOAA/HRD HWIND analysis patched in for the storm region. HWIND vector wind fields are first patched into COAMPS wind fields, and then wind stress is calculated using bulk formula with the Donelan *et al.* (2004) drag coefficient prior to model runs. The model is nested within a GOM data-assimilative hindcast that uses the U. S. Navy NCODA system. It is run with 26 vertical layers and KPP vertical mixing is used. Surface turbulent fluxes are calculated during the model run using the COARE 3.0 algorithm bulk formula. The remaining experiments all differ from GOM1 by altering one single model attribute (Table 1). GOM2 isolates sensitivity to horizontal resolution, GOM3 and GOM4 to vertical resolution, GOM5 and GOM6 to vertical mixing scheme, GOM7-GOM11 to wind stress drag coefficient parameterization, GOM12 to turbulent heat flux drag coefficient representation, GOM13 to surface forcing resolution (COAMPS without HWIND patching), GOM14 to ocean model initialization (nesting within a non-assimilative ocean model), and GOM15 to one-dimensional (1-D) ocean dynamics.

Model Attribute	Recommendations
Horizontal resolution	≈10 km adequately resolves horizontal structure of response forced by eye/eyewall
Vertical resolution	≈10 m in the OML is adequate to resolve vertical structure of shear
Vertical mixing	KPP outperformed the other models; MY, GISS produce slower cooling, larger heat flux, less-accurate shear representation
$C_D$	Donelan, Large & Pond capped, Jarosz <i>et al.</i> (values between 2.0 and $2.5 \times 10^{-3}$ at high wind speed) produce most realistic results
$C_{EL}, C_{ES}$	Little SST and velocity sensitivity but large heat flux sensitivity. Need heat flux observations to evaluate
Atmospheric forcing	Must resolve inner-core structure ( $\leq 10$ km horizontal resolution)
Outer model (assimilative vs. non-assimilative)	Accurate initialization is the most important factor to accurately forecast velocity and SST evolution
Ocean dynamics (1-D vs. 3-D)	3-D required (second most important factor in the GOM)

**Table 2:** Recommendations to improve upper-ocean forecasts of SST evolution during tropical cyclones based on analysis of the simulated ocean response to Hurricane Ivan in the Gulf of Mexico (Halliwell *et al.*, 2010)

Forecast sensitivity and accuracy was evaluated by focusing on the responses of SST, surface turbulent heat flux beneath the storm, and upper-ocean velocity (Halliwell *et al.* 2010). The latter response to hurricane Ivan was evaluated against an ADCP mooring array deployed over the northern Gulf of Mexico shelf/slope region as part of the *Slope to Shelf Energetics and Exchange*

*Dynamics (SEED)* project (Teague *et al.* 2005) that was directly hit by Ivan. Recommendations based on these studies are summarized in Table 2.

**SST Response Evaluation:** Halliwell *et al.* (2010) evaluate the simulated SST cooling patterns forced by Ivan against daily SST fields generated by the objective analysis of *in-situ* observations along with AVHRR and microwave satellite observations onto a 0.25° global grid (Reynolds *et al.*, 2007), hereinafter referred to as “blended” SST. The mean differences listed in Table 3 demonstrate that in the subdomain over which these analyses were performed, the ocean model did not cool as much as indicated by the blended SST fields. Although the model overcooled within a cold-core cyclone centered near 25°N, 87°W by >4°C (Halliwell *et al.*, 2010), this overcooling was more than compensated for by undercooling over the remainder of the domain. Mean differences display the largest sensitivity to ocean model initialization, surface forcing resolution, and wind stress drag coefficient, with more (less) cooling occurring for larger (smaller) values of  $C_D$ . Smaller sensitivity is evident for vertical mixing choice, with the MY and GISS schemes producing slightly more cooling than KPP. Little sensitivity is evident to vertical and horizontal resolution. RMS differences between the simulations and blended SST are substantially increased by the large simulated overcooling in the cold-core cyclone centered near 25°N, 87°W.

Table 3. Comparison of  $\Delta T$  (forced by Ivan) images (17 Sept. minus 10 Sept.) between the 15 experiments and blended SST: mean difference (column 2) and RMS difference (column 3)

Experiment	$\Delta T$ Mean Difference (°C)	$\Delta T$ RMS Difference (°C)
GOM1	0.24	1.33
GOM2	0.25	1.29
GOM3	0.30	1.40
GOM4	0.22	1.40
GOM5	0.30	1.26
GOM6	0.47	1.33
GOM7	0.38	1.33
GOM8	0.04	1.57
GOM9	0.14	1.47
GOM10	-0.19	1.71
GOM11	0.06	1.37
GOM12	0.11	1.34
GOM13	0.51	1.24
GOM14	0.84	1.51
GOM15	0.06	1.55

Halliwell *et al.* (2010) further evaluate the fidelity of simulated SST cooling patterns using advanced analysis techniques, specifically Taylor (2001) diagrams and the Murphy (1988) skill scores (not shown). Summarizing the overall conclusions, the control experiment produced one of the most realistic SST response patterns as expected. Three experiments stood out as much inferior to the control experiment, specifically GOM13 (low-resolution atmospheric forcing,

GOM14 (alternate initialization) and GOM15 (one-dimensional ocean dynamics). All other experiments produced SST cooling patters that were equally correlated with cooling in the blended analysis ( $\approx 0.7$ ), but some of the wind stress drag coefficient choices degraded the realism of the cooling response. Drag coefficient values substantially smaller than the Donelan choice used in the control experiment tended to underestimate the magnitude of the cooling pattern (GOM7) while values substantially larger than Donelan substantially overestimated the magnitude of the cooling pattern (GOM8, GOM10). The quality of the eight other experiments was almost identical to the quality of the control experiment. However, this does not mean that all of the model attributes evaluated in these eight experiments will have an insignificant influence on storm intensity. For example, although the SST cooling pattern was only slightly different among the three vertical mixing choices (GOM1, GOM5, GOM6), they produced potentially significant differences in the turbulent heat flux from ocean to atmosphere (up to  $200 \text{ W m}^{-2}$ ) beneath the inner core of the storm. Although changing the surface turbulent heat flux parameterization (GOM12) had little influence on the SST cooling pattern, it also had a potentially significant influence on the heat flux (differences up to  $300 \text{ W m}^{-2}$ ). Further details on model evaluation are contained in Halliwell *et al.* (2010).

**Measurements:** Hurricane Ivan passed directly over 14 ADCP moorings that were deployed as part of the NRL *Slope to Shelf Energetics and Exchange Dynamics (SEED)* project from May through Nov 2004 (Teague *et al.* 2007) (Figure 1). These observations enable the simulated ocean current (and shear) response to a hurricane over a continental shelf/slope region to be evaluated. This evaluation also involves detailed comparisons between *in-situ* and satellite-derived OHC estimates based on Surface Height Anomaly (SHA) fields from available radar altimeters (NASA TOPEX, Jason-1, ERS-2, NOAA GEOSAT Follow-On-Missions), and infrared and microwave SSTs from TRMM and AMSR-E.

Table 4: Summary of measurements from four of the fourteen NRL SEED ADCP arrays (LR-Long Ranger, TRBM- Trawl Resistant Bottom Mount) spanning the coastal ocean (60 m) to the continental slope (1029 m). For the purposes of this brief report we will focus on Array 8 and 9 as they were located along Ivan’s track (8) and at  $1.5 R_{\max}$  (9) to the right of the track.

Array #	Lat °N	Long °W	Start Date 2004	End Date 2004	$\Delta t$ (hr)	Depth Range (m)	$\Delta z$ (m)	Bottom Depth (m)	Instrument Type
2	29.43	88.01	05/01	10/31	<b>0.25</b>	4-54	<b>2</b>	<b>60</b>	TRBM
8	29.14	88.11	05/03	11/07	<b>1.0</b>	42-492	<b>10</b>	518	LR
9	29.19	87.94	05/03	11/07	<b>1.0</b>	40-500	<b>10</b>	518	LR
14	29.20	87.65	05/05	11/07	<b>1.0</b>	42-502	<b>10</b>	<b>1029</b>	LR

**Current Profiler Analyses:** As shown in Table 4, a synopsis of four of the fourteen ADCP arrays are summarized with respect to position, range of measurements temporal vertical sampling intervals as discussed by Teague *et al.* (2007). These profiler measurements provided the evolution of the current (and shear) structure from the deep ocean across the shelf break and over the continental shelf. The current shear response, estimated over 4-m vertical scales, is shown in Figure 2 based on objectively analyzed data from these moorings. Over the shelf, the current shears increased due to hurricane Ivan strong winds. The normalized shear magnitude is a factor of four times larger over the shelf (depths of 100 m) compared to normalized values over

the deeper part of the mooring array (500 to 1000 m). Notice that the current shear rotates anticyclonically (clockwise) in time over 6-h intervals consistent with the forced near-inertial response (periods slightly shorter than the local inertial period). In this measurement domain, the local inertial period is close to 24 h which is close to the diurnal tide. By removing the weaker tidal currents and filtering the records, the analysis revealed that the predominant response was due to forced near-inertial motions. These motions have a characteristic time scale for the phase of each mode to separate from the wind-forced OML current response when the wind stress scale ( $2R_{max} \sim 64$  km in Ivan during time of closest approach) exceeds the deformation radius associated with the first baroclinic mode ( $\approx 30$  to  $40$  km). This time scale increases with the number of baroclinic modes due to decreasing phase speeds (Shay *et al.* 1998). The resultant vertical energy propagation from the OML response is associated with the predominance of the anticyclonic (clockwise) rotating energy with depth and time that is about four times larger than the cyclonic (counterclockwise) rotating component.

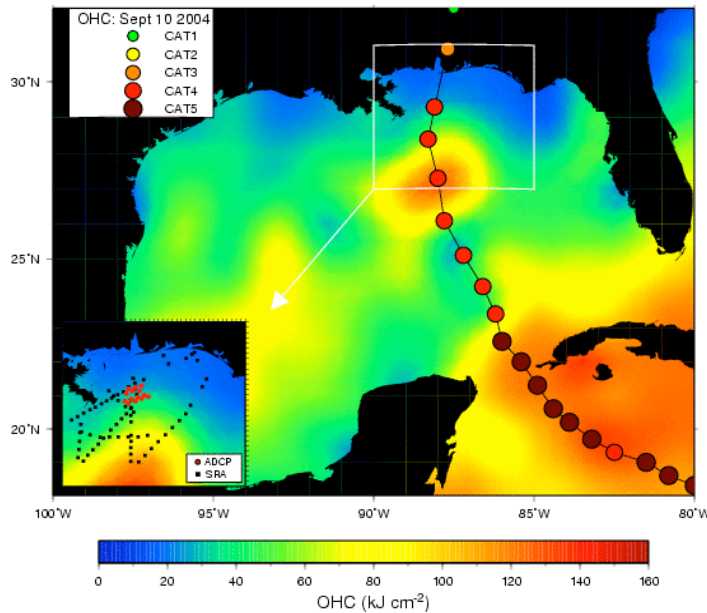


Figure 1: OHC map and inset showing NRL mooring locations (red) and SRA wave measurements (black) relative to Ivan's storm track and intensity. The OHC pattern shows the WCR encountered by Ivan prior to landfall. The cooler shelf water ( $OHC < 20$  kJ cm<sup>-2</sup>) resulted from the passage of Frances two weeks earlier.

Observed current shear profiles were estimated over 4-m vertical scales for each time sample following hurricane passage at arrays 8 and 9 are shown in Figure 3. Notice that the shear magnitudes are typically two to three times larger than observed in the Loop Current during Lili's passage. This is not surprising since these measurements were acquired in the Gulf Common Water (Nowlin and Hubertz, 1972) and similar to those documented during hurricane Gilbert's passage where up to 3.5°C cooling was observed. In the near-inertial wave wake (Shay *et al.*, 1998), the key issue is how much of the current shear is associated with near-inertial wave processes. Compared to the Gulf Common Water, the presence warm and cold eddies significantly impact these levels of near-inertial wave (and shear) activity (Jaimes and Shay, 2010). This is now being explored prior to comparing these values to those from the HYCOM model for each of the experiments discussed above.

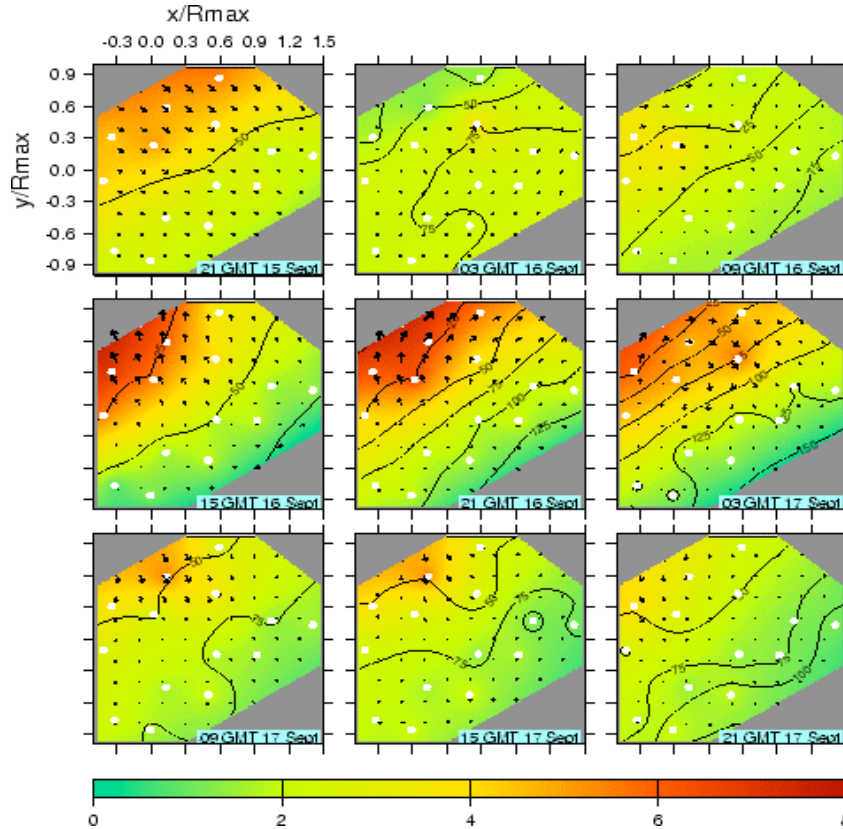


Figure 2: Spatial evolution of the rotated current shear magnitude normalized by observed shears from the ADCP measurements (white dots) normalized by observed shears in the Loop Current of  $1.5 \times 10^{-2} \text{ s}^{-1}$  (color) during Lili starting at 2100 GMT 15 Sept every 6 hours. Black contours (25-m intervals) represent the depth of the maximum shears based on the current profiles from the moored ADCP. Cross-track (x) and along-track (y) are normalized by the Rmax of 32 km.

**Model versus Observed Current Shear Comparisons:** At mooring 9 (Figure 4), velocity shear magnitudes from the control experiment GOM1 are compared to the shear profiles over the upper 150 m. Good agreement exists between observed and simulated current shears from KPP with the Donelan *et al.* drag coefficient over the first two inertial periods. These observations and simulations suggest vertical energy propagation out of the surface mixed layer and into the thermocline consistent with surface intensified flows (Jaimes and Shay 2010). Velocity shear comparisons clearly reveal differences among the three vertical mixing schemes evaluated in GOM1, GOM5, and GOM6. Central to the momentum flux issue (e.g., surface drag coefficient), GOM1, GOM7 and GOM8 are also compared with respect to the forced current shear structure (right panels in Figure 4). The Donelan *et al.*  $c_d$  seems to produce the most realistic shear profile in the upper 150 m compared to the Powell (GOM7) and the Large and Pond (GOM8) formulations. Based on these comparisons, KPP mixing scheme with the Donelan drag coefficient are the schemes of choice for the Ivan data set. We are in the process of making such comparisons for all the ADCP records during storm forcing. The import of this surface drag cannot be over stated in that the surface stress drives the current and its shear that will lead to enhanced shear instabilities and entrainment mixing. So these schemes are clearly linked in obvious and subtle ways (Halliwell *et al.* (2010).

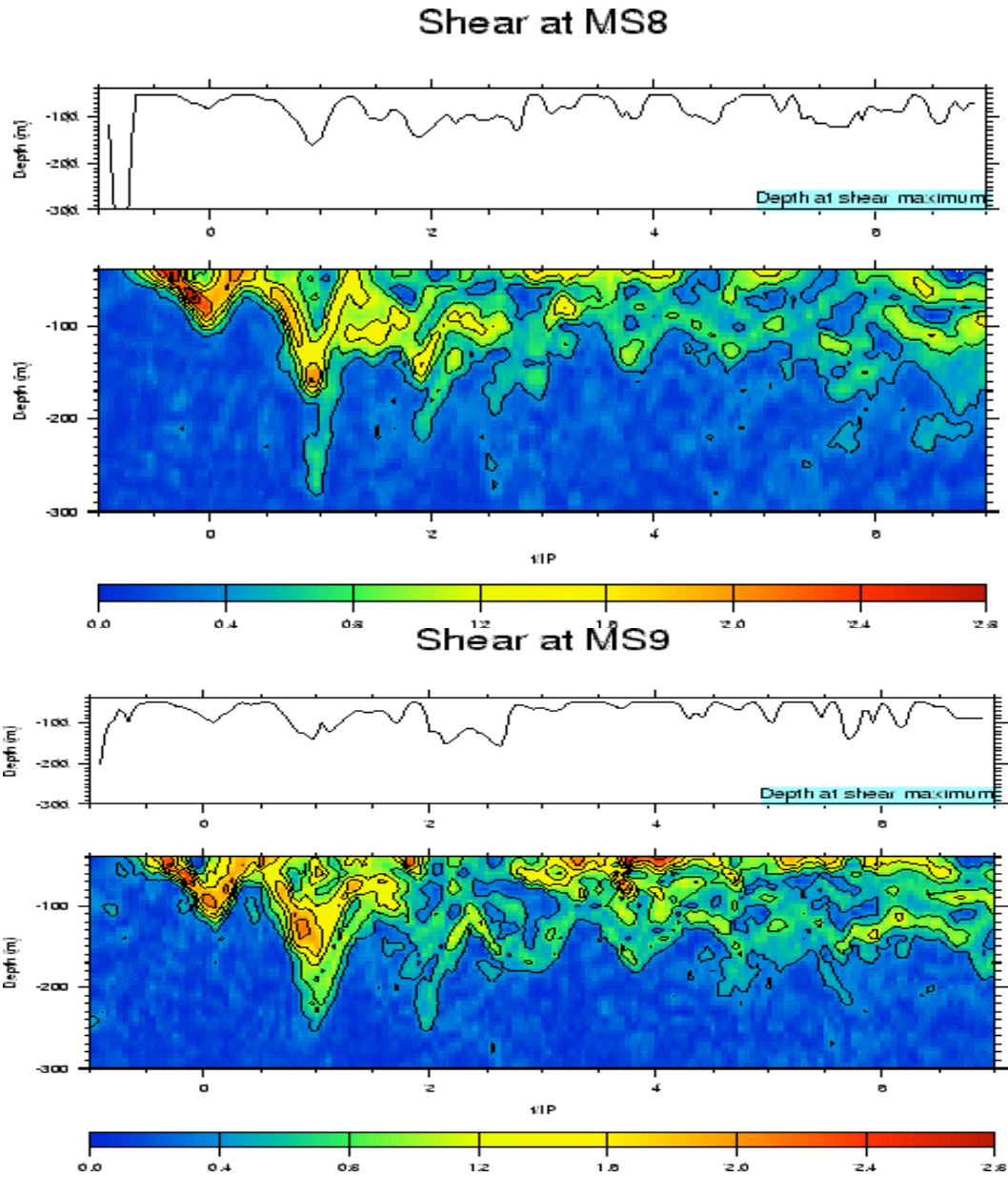
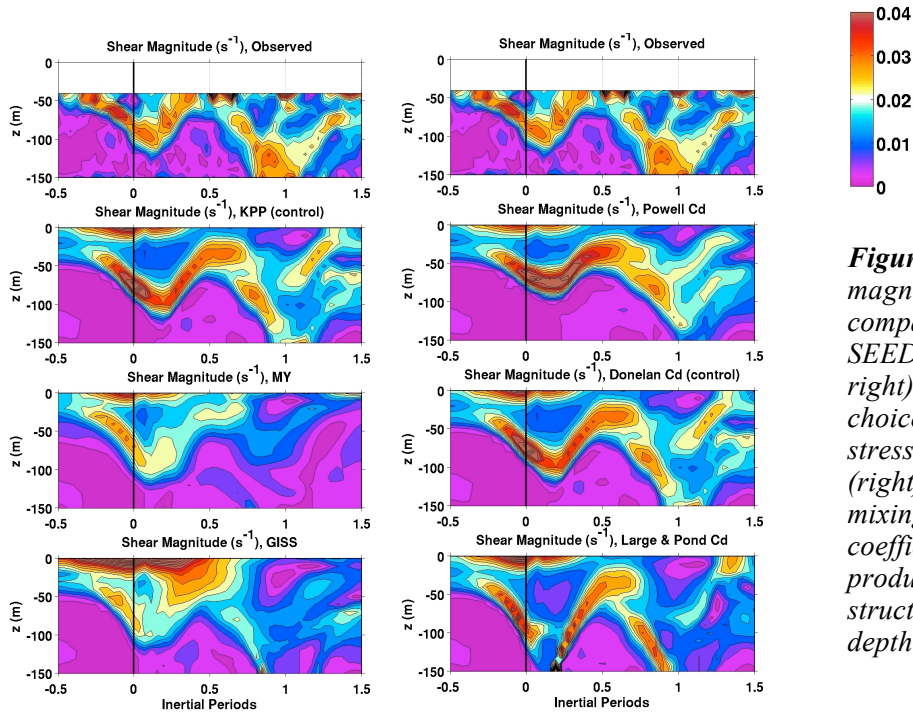


Figure 3: Time series (normalized by inertial period) of observed current shear magnitudes (colored contours) and the respective depths (m) of maximum current shears observed at Moorings 8 (upper: along Ivan's track) and 9 (lower:  $1.5 R_{\max}$  to the right of the Ivan) relative to the time of the closest approach. Shears are normalized by a value of  $1.5 \times 10^{-2} \text{ s}^{-1}$  that have been observed in the Loop Current (Shay and Uhlhorn, 2008).



**Figure 4:** Time series of the magnitude of vertical shear ( $s^{-1}$ ) comparing observations from SEED mooring 9 (top left and top right) to three vertical mixing choices (left) and three wind stress drag coefficient choices (right). The combination of KPP mixing and Donelan et al. drag coefficient parameterizations produce the most realistic shear structure and maximum OML depth.

**Interactions with NOAA/NCEP/EMC:** A major goal of this project is to interact with the HWRP developers at EMC and URI to evaluate the performance of ocean models to be used in the next-generation HWRP model and to improve the performance of the ocean model. As part of this effort, we started to work on the presumed cooling of warm core eddies of several degrees as suggested by Yablonsky and Ginis (2009). In this context, URI provided feature-based initialization fields to G. Halliwell initially to be used in a POM-HYCOM comparison study. As part of our effort under this JHT project to improve ocean model performance in hurricane forecasts, we are comparing the impact of different ocean initialization products (an important objective) on the accuracy of SST forecasts. We discovered the problems described as we were preparing the feature-based fields to initialize HYCOM simulations of the ocean response to Ivan, Katrina, and Rita.

The primary problem can be stated simply with the POM-HYCOM initialization: Baroclinic fronts slope in the wrong direction with increasing depth. This situation is illustrated by initial HYCOM fields prior to hurricane Ivan produced from the feature-based product and spun up for several inertial periods. Figure 5 shows the SSH pattern in the Gulf of Mexico, highlighting the LC Path and the detached warm ring. The subsurface structure of these features is investigated along the two sections shown in Figure 5. A meridional cross-section of zonal velocity through the warm ring (Figure 6) reveals that the diameter of the ring *increases* with increasing depth instead of decreasing as expected. Similarly, a zonal cross-section of meridional velocity across the Loop Current north of the Yucatan Channel (Figure 6) demonstrates that the core of maximum velocity shifts *westward* with increasing depth instead of eastward as expected. In both of these sections, the model interfaces below the near-surface level-coordinate domain follow isopycnals and demonstrate that the fronts (large horizontal density gradient and vertical shear) slope in the wrong direction with increasing depth. There is also a problem in blending the

ring with the background ocean structure that is manifested by the large vertical density jump near 650 m depth in the ring interior.



Figure 5. Pre-Ivan initial SSH map derived from the feature-based ocean model initialization product. The two cross-sections presented in Figure 6 are illustrated with black bars.

<b>Flight</b>	<b>AXBT</b>	<b>AXCP</b>	<b>AXCTD</b>	<b>TOTAL</b>
100508H	52 (48)	0	0	52 (48)
100518H	29 (28)	26 (10)	11 (10)	66 (48)
100521H	42 (39)	22 (11)	2 (2)	66 (52)
100528H	41 (37)	22 (9)	2 (1)	63 (47)
100603H	37 (34)	23 (11)	6 (6)	66 (51)
100611H	53 (49)	15 (10)	0	68 (59)
100618H	34 (23)	22 (8)	8 (7)	63 (38)
100625H	58 (53)	0	6 (6)	64 (59)
100709H	59 (54)	12 (12)	6 (3)	77 (69)
<b>TOTAL</b>	<b>405 (365)</b>	<b>142 (71)</b>	<b>41 (35)</b>	<b>588 (471)</b>

Table 5: Summary of nine NOAA WP-3D aircraft flights on RF-42 in the eastern Gulf of Mexico from 24 to 28°N and 85 to 89°W in support of Deep Water Horizon Oil Well Spill that occurred on 20 April 2010 in the northern Gulf of Mexico along the slope of the DeSoto Canyon . The overall success rate for all probes (in parentheses) was 80.1%. This is lower than usual due to manufacturing problems with the AXCPs such as unsealed transmitter boards, agar, and software and firmware problems in the new Mark21/Mark10A software. The number of GPS sondes deployed was 78 with 95% success rate to help reduce flight level winds to the surface.

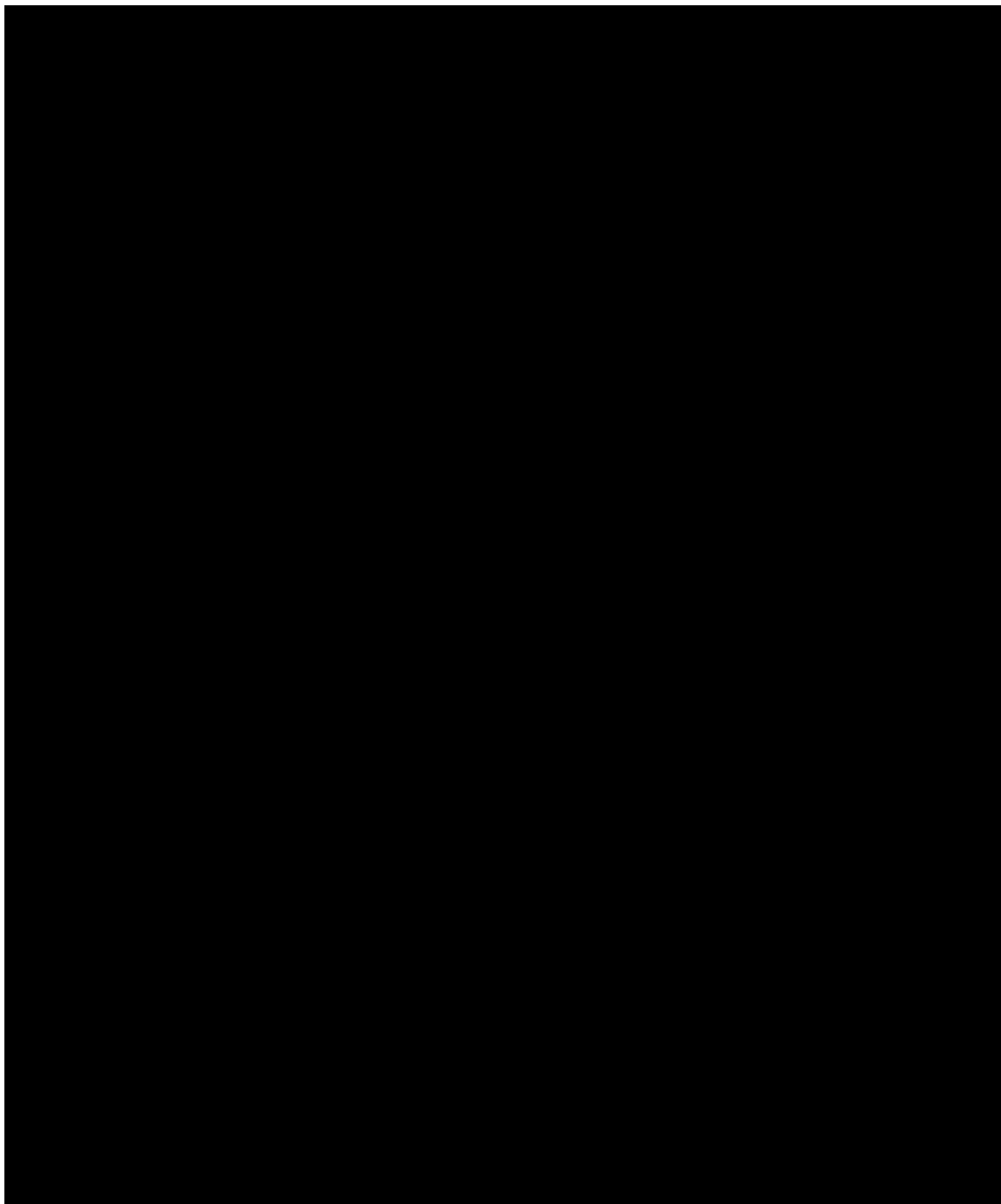


Figure 6. Pre-Ivan velocity cross-sections: (top) zonal velocity from a meridional section through the detached ring and (bottom) meridional velocity from a zonal section across the Loop Current. The locations of these two cross-sections are illustrated in Figure 5.

**DeepWater Horizon Oil Spill:** The effort to improve ocean model initialization will be significantly enhanced by our emergency effort to improve ocean model products in response to the Deepwater Horizon oil spill. Since early May of this year, both Shay and Halliwell have redirected a large part of their work toward observational and modeling efforts in response to the Deepwater Horizon oil spill. For Shay, this has involved flying nine missions from the NOAA WP-3D research aircraft to sample the Loop Current and adjacent eddies over the eastern Gulf of Mexico by deploying AXBTs, AXCPs and AXCTDs and GPS sondes (~666 profilers) in support of oil spill forecasting (see Table 5). Much of this sampling grid was over the MMS moorings deployed in support of the Loop Current Dynamics Study. Halliwell redirected most of his modeling efforts to GOM modeling in support of oil spill forecasting. The short-term effect of this emergency effort was to delay our underway analysis of other storms (Katrina, Rita, Frances, Gustav, Ike). In the longer term, however, this work will provide extensive benefits to this proposed continuation project. The repeated aerial sampling over the eastern GOM provides an unprecedented dataset for evaluating ocean model products that will lead to significant improvements in our ability to accurately initialize ocean models for coupled hurricane forecasting. Furthermore, the emergency aircraft sampling revealed significant problems with many of the AXCP probes and with aircraft receivers that should lead to improved sampling in the future in support of IFEX and HFIP.

Due to the high value of these P3 observations (see Figure 7) along with other special observations (cruise profiles, surface drifters) acquired in response to the oil spill in conjunction with existing MMS moored measurements, we will initially focus our evaluation of the ocean nowcast-forecast products being used to initialize the ocean model on the 2010 storm season whether or not a hurricane actually strikes the region. Product evaluation will focus on the HYCOM products available from NRL-Stennis and NAVO along with the NCEP/EMC RTOFS. As this study progresses, we will gradually restart the product evaluation work during the other storms. In addition to evaluation efforts, we will perform Observing System Experiments (OSEs) to quantify the impact of both existing operational observations and special targeted observations on the quality of initial ocean fields, and Observing System Simulation Experiments (OSSEs) to identify enhancements to the existing observing system that will reduce initialization errors to tolerable levels. This comprehensive work should allow unambiguous identification of the optimum ocean products for initialization among those presently available while identifying improvements to observational coverage that may be necessary to further reduce initialization errors.

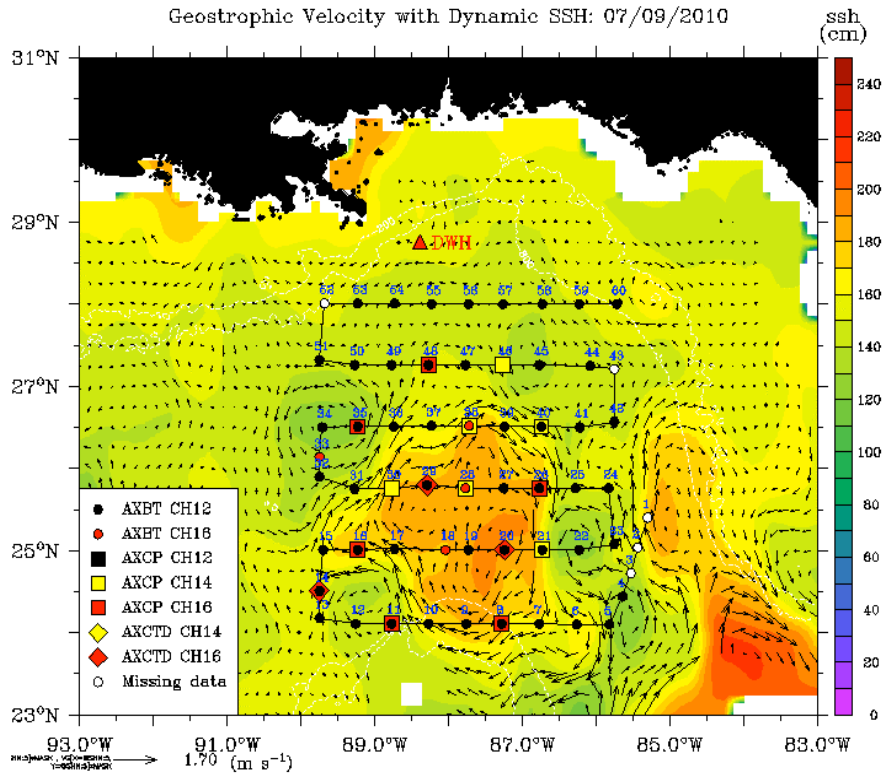


Figure 7: NOAA WP-3D mesoscale ocean grid on 9 July 2010 deploying a combination of AXBTs (circles), AXCTDs (diamonds), and AXCPs (squares) superposed on sea surface height (cm: color bar) and surface geostrophic currents based on sea surface slopes (maximum vector is  $1.7 \text{ m s}^{-1}$ ). Notice that warm core eddy (called Franklin) detached from the Loop Current.

**Katrina and Rita:** The 3-D upper ocean thermal and salinity structure in the LC system was surveyed with Airborne eXpendable BathyThermographs (AXBT), Current Profilers (AXCP), and Conductivity-Temperature-Depth sensors (AXCTD) deployed from four aircraft flights during September 2005, as part of a joint NOAA and National Science Foundation experiment (Rogers *et al.*, 2006; Shay, 2009). Flight patterns were designed to sample the mesoscale features in the LC system: the LC bulge (amplifying WCE), the WCE that separated from the LC about two days before the passage of Rita, and two CCEs that moved along the LC periphery during the WCR shedding event (Fig. 8). The first aircraft flight was conducted on 15 Sept (two weeks after Katrina or one week before Rita, i.e. pre-Rita), the second and third flights were conducted during Rita's passage (22 and 23 Sept, respectively), and the final flight was conducted on 26 Sept, a few days after Rita's passage. Pre-Rita and post-Rita (not shown) flights followed the same pattern, while these other Rita flights focused on different regions along Rita's track. Data acquired during pre-Rita includes temperature profilers from AXBTs, temperature and salinity profilers from AXCTDs, and current and temperature profilers from two AXCPs deployed in the western and eastern sides of the WCE (Jaimes and Shay 2009). A salient characteristic of the WCE is the salinity maximum of  $\sim 36.4$  to  $36.7$  practical salinity units. This behavior must be incorporated into numerical models, as a climatological salinity profile is insufficient to accurately initialize an model ocean with a WCE. Realistic salinity profiles to match the temperature profiles would then resolve horizontal density gradients and the corresponding geostrophic flows associated with oceanic features (Shay *et al.*, 1998).

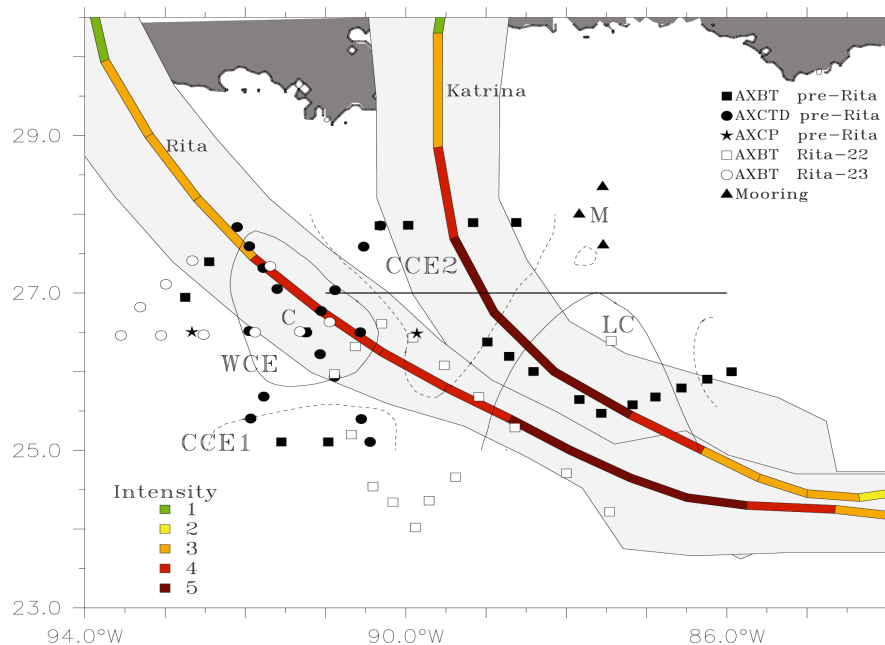


Figure. 8: Airborne profilers deployed in Sept 2005 relative the track and intensity of Katrina and Rita (colored lines, with color indicating intensity as per the legend) over the LC System. The light-gray shades on the sides of the storm tracks represent twice the radius of maximum winds ( $R_{max}$ ). The contours are envelopes of anticyclonic (solid: WCE and LC) and cyclonic (dashed: CCE1 and CCE2) circulations. A set of AXBTs (not shown) was deployed after hurricane Rita (26 Sept), following a sampling pattern similar to pre-Rita (or post Katrina) (15 September). Point M indicates the position of several MMS moorings used during this study, and Point C represents the drop site for profiler comparison (AXBT versus AXCTD). The transect along 27°N indicates the extent of vertical sections discussed in the text (Jaimes and Shay 2009).

The combination of these airborne profiles of temperature and salinity measurements with the MMS-sponsored ADCP and CTD moorings were fairly consistent. These continuous measurements of ocean temperatures, salinities (via conductivities), and currents were acquired from the mooring sensors at intervals of 0.5 and 1 hr for CTDs and ADCPs, respectively. Although the moorings were located outside the radius of maximum winds  $R_{max}$  of hurricanes Katrina ( $\sim 4.5 R_{max}$  where  $R_{max} = 47$  km) and Rita ( $\sim 17.5 R_{max}$  where  $R_{max} = 19$  km) (Fig. 8), CCE2 that was affected by Katrina (category 5 status) propagated over the mooring site  $\approx 2$  days after interacting with the storm. The circulation of the LC bulge that interacted with Rita (category 5 status) extended over the mooring  $\approx 3$  days after having been affected by the storm. The cluster averages of the thermal structure revealed that the LC cooled by 1°C, the WCE temperature cooled by 0.5°C, and the eddy shedding region and the CCE cooled by more than 4.5°C (Jaimes and Shay 2009). These profiles will represent a challenge for the model especially placing the oceanic features in the correct position as suggested by the Ivan model analyses (Halliwell *et al.*, 2010).

Jaimes and Shay (2010) analyzed the contrasting thermal responses during and subsequent to Katrina and Rita by estimating the energetic geostrophic currents in these oceanic features. Increased and reduced oceanic mixed layer (OML) cooling was measured following the passage

of both storms over cyclonic (CCE) and anticyclonic (WCE) geostrophic relative vorticity  $\zeta_g$ , respectively (Fig. 9). Within the context of the storms' near-inertial wave wake in geostrophic eddies, ray-tracing techniques in realistic geostrophic flow indicate that hurricane forced OML near-inertial waves are trapped in regions of negative  $\zeta_g$ , where they rapidly propagate into the thermocline. These anticyclonic-rotating regimes coincided with distribution of reduced OML cooling, as rapid downward dispersion of near-inertial energy reduced the amount of kinetic energy available to increase vertical shears at the OML base. By contrast, forced OML near-inertial waves were stalled in upper layers of cyclonic circulations, which strengthened vertical shears and entrainment cooling. Upgoing near-inertial energy propagation dominated inside a geostrophic cyclone that interacted with Katrina; the salient characteristics of these upward propagating waves were: (i) radiated from the ocean interior due to geostrophic adjustment following the upwelling and downwelling processes; (ii) rather than with the buoyancy frequency, they amplified horizontally as they encountered increasing values of  $\zeta_g$  during upward propagation; (iii) produced episodic vertical mixing through shear-instability at a critical layer underneath the OML. To improve the prediction of TC-induced OML cooling, models must capture geostrophic features; and turbulence closures must represent near-inertial wave processes such dispersion and breaking between the OML base and the thermocline. Oceanic response models must capture this variability to get the correct entrainment in cold and warm oceanic features. For the first time, these effects of the near-inertial wave wake in the presence of a background eddy field are now being explored in this study using these measurements and results from analytical theory.

**Gustav and Ike:** Hurricanes Gustav and Ike moved over the Gulf of Mexico and interacted with the LC and the eddy field in August and September 2008. As part of the NCEP tail Doppler Radar Missions, oceanic and atmospheric measurements were acquired on sixteen NOAA WP-3D research flights for pre, during and post-storm flights. In total, over 400 AXBTs and 200 GPS sondes were deployed to document the evolving atmospheric and oceanic structure over warm and cooler ocean features in these two hurricanes (Table 6). In addition, forty-five GPS sondes were deployed on 1 Sept over the float and drifter array deployed by the United States Air Force WC-130J north and west of the Loop Current. Similar to CBLAST observations, the float array also included the EM/APEX floats that measure the horizontal velocities as well as temperature and salinity structure (Sanford *et al.*, 2007). However, this effort significantly improved upon the CBLAST effort in that the forcing is better documented with the combination of GPS sondes and the Stepped Frequency Microwave Radiometer (Uhlhorn *et al.*, 2007) directly over the float and drifter array. In addition, each research flight carried AXBTs to document the evolving upper ocean thermal structure across the entire Gulf of Mexico for the first time. Note that the AXBTs were deployed to document pre- and post-storm oceanic variability in the Loop Current and its periphery where float and drifter measurements would be advected away from the storm track by the energetic ocean current. This is precisely why we need current profilers to deploy from the research aircraft on a routine basis.

**Summary:** We made progress on this grant as the numerical simulations with ocean conditions observed during hurricane Ivan's passage by Walker *et al.* (2005). Warm and cold eddies suggest regimes of less and more negative feedback to the atmosphere. We have completed the analysis of Ivan within the context of mixing and upwelling and downwelling processes by comparing simulations of the currents and shears to *in situ* measurements from the SEED moorings (Teague *et al.*, 2007). In addition, we have analyzed pre- Katrina and Rita observations including detailed ray-tracing techniques to demonstrate the markedly different character of the forced near-inertial motions (Jaimes 2009; Jaimes and Shay 2010). We will conduct a similar analysis on the model

simulations to assess the impact on the mixing schemes via shear-instability. Such combined numerical and observational efforts here have benefitted from a PhD student (B. Jaimes) to examine model sensitivities and comparing these simulations to the NRL and MMS profiler measurements. Given the 5-year program of the recently funded MMS Dynamics of the Loop Current Study (\$7M), this project will benefit significantly from in-situ mooring data as well as the detailed aircraft measurements that will be acquired during the NOAA IFEX, NASA GRIP, and NSF PREDICT experiments during the summer of 2010. In addition, the nine successful flights in support of DW Horizon Oil Spill will certainly improve ocean model initialization at EMC over the longer term as a warm eddy was shed from the Loop Current over that three month period. This is a regime where hurricanes can rapidly weaken or deepen as they interact with both warm and cold ocean features. Even under quiescent conditions, these data sets will represent a challenge to the model to get the 3-D temperature, salinity and current structure accurately through vertical projection of the altimetry data. Finally processed profiler data from Gustav and Ike flights are being synthesized with drifter and float data to provide a clearer description of the cold wake northeast of the Loop Current where cooling exceeded 3°C compared to the Loop Current of about 1°C.

Table 6: Summary of atmospheric (GPS) and oceanic (AXBT) profiler measurements from sixteen flights acquired in hurricanes Gustav and Ike in 2008. Numbers in parentheses represent profiler failures.

Hurricane Gustav				Hurricane Ike			
Date	Flight	GPS	AXBT	Date	Flight	GPS	AXBT
(2008)				(2008)			
28 Aug	RF43	0	49(2)	08 Sep	RF43	0	47(2)
29 Aug	RF42	12(4)	16(0)	09 Sep	RF42	19	6(0)
30 Aug	RF43	9	19(2)	10 Sep	RF42	17(1)	10(2)
31 Aug	RF42	24	16(1)	10 Sep	RF43	11	20(7)
31 Aug	RF43	17(2)	19(1)	11 Sep	RF42	16	10(1)
01 Sep	RF43	44	19	11 Sep	RF43	10	22(3)
03 Sep	RF43	4	54(4)	12 Sep	RF42	21(2)	10(4)
				12 Sep	RF43	8	20(4)
				15 Sep	RF43	0	61(5)
Total	7	111(6)	191(10)		9	111(3)	216(28)

**Acknowledgments:** This study has benefited from the interactions with Mr. William Teague in the Oceanography Department at the US Naval Research Laboratory at Stennis Space Center, Dr. Alexis Lugo-Fernandez at Minerals Management Service sponsored ADCP moorings. This project has also benefited from continuing support from the National Science Foundation (Dr. Stephen Nelson) in the acquisition and analysis of measurements acquired during hurricanes in collaboration with NOAA’s Hurricane Research Division (Drs. Frank Marks, Rob Rogers, Eric

Uhlhorn) and Aircraft Operations Center (Dr. James McFadden). Dr. Benjamin Jaimes also contributed to this effort.

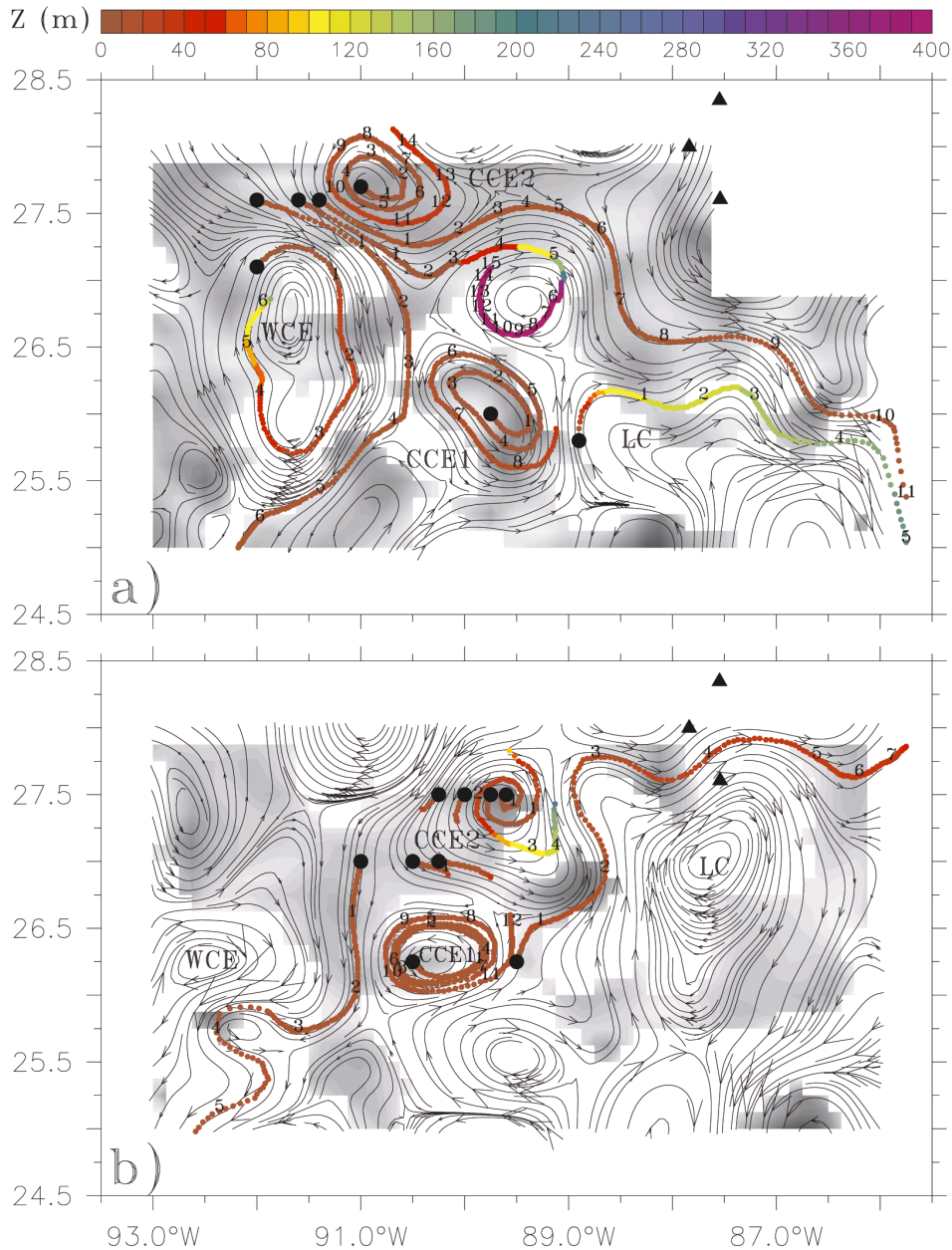


Figure 9: Near-inertial wave ray-tracing based on Kunze's (1985) model, for (a) Katrina and (b) Rita. The numbers along the wave rays indicate inertial periods (one inertial period is  $\sim 25.5$  hr), dots are hourly positions, color is the ray's depth level, and the flow lines are from geostrophic flow fields derived from (a) post Katrina (15 Sept.) and (b) post Rita (26 Sept.) airborne-based data. The gray shades represent regions where the effective Coriolis parameter exceeds  $> 0.2$ . This ratio, and the flow lines were calculated from depth-averaged velocity fields.

**References and Publications :**

- Donelan, M. A., B. K. Haus, N. Reul, W. J. Plant, M. Stiassine, H. Graber, O. Brown, and E. Saltzman, 2004: On the limiting aerodynamic roughness of the ocean in very strong winds. *Geophys. Res. Letters.*, 31L18306,doi:1029/2004GRL019460.
- \*Halliwell, G., L. K. Shay, S. D. Jacob, O. Smedstad, and E. Uhlhorn, 2008: Improving ocean model initialization for coupled tropical cyclone forecast models using GODAE nowcasts. *Mon. Wea Rev.*, 136 (7), 2576–2591.
- \*Halliwell, G. R., L. K. Shay, J. Brewster, and W. J. Teague. 2010: Evaluation and sensitivity analysis to an ocean model response to hurricane Ivan. *Mon. Wea. Rev.* **(In Press)**
- \*Jaimes, B., 2009: On the oceanic response to tropical cyclones in mesoscale ocean eddies. PhD Dissertation. Division of Meteorology and Physical Oceanography, Rosenstiel School of Marine and Atmospheric Science, University of Miami, Miami, FL 33149, 143 pp.
- \*Jaimes, B. and L. K. Shay. 2009: Mixed layer cooling in mesoscale eddies during Katrina and Rita. *Mon. Wea. Rev.*, **137**, 4188–4207.
- \*Jaimes, B. and L. K. Shay, 2010: Near-inertial wave wake of hurricanes Katrina and Rita in mesoscale eddies. *J. Phys. Oceanogr.* . . *J. Phys. Oceanogr.*, **40(6)**, 1320-1337.
- Jarosz, E., D. A. Mitchell, D. W. Wang, and W. J. Teague, 2007: Bottom-up determination of air-sea momentum exchange under a major tropical cyclone. *Science*, 315, 1707-1709.
- \*Mainelli, M., M. DeMaria, L. K. Shay and G. Goni. 2008: Application of oceanic heat content estimation to operational forecasting of recent category 5 hurricanes, *Wea and Forecast.*, 23(1), 3-16.
- Murphy, A. H., 1988. Skill scores based on the mean square error and their relationships to the correlation coefficient. *Mon. Wea. Rev.*, **116**, 2417-2424.
- Nowlin, W. D. Jr., and J. M. Hubertz, 1972: Contrasting summer circulation patterns for the eastern Gulf. In: *Contributions on the Physical Oceanography of the Gulf of Mexico, Tex. A&M Oceanogr. Stud.*, vol. 2, edited by L. R. A. Capurro and J. L. Reid, pp. 119-138, Gulf Pub. Co.
- Reynolds, R. W., T. M. Smith, C. Liu, D. B. Chelton, K. S. Casey, and M. G. Schlax, 2007: Daily high-resolution blended analyses for sea surface temperature. *J. Climate*, **20**, 5473-5496.
- Rogers, R., S. Abernethy, M. Black, P. Black, J. Cione, P. Dodge, J. Dunion, J. Gamache, J. Kaplan, M. Powell, L. K. Shay, N. Surgi, E. Uhlhorn, 2006: The intensity forecasting

experiment (IFEX), a NOAA multiple year field program for improving intensity forecasts. *BAMS*, 87(11), 1523-1537.

\*Rappaport, E. N., J. L. Franklin, M. DeMaria, A. B. Shumacher, L. K. Shay and E. J. Gibney, 2010: Tropical cyclone intensity change before U. S. Gulf coast landfall. *Wea. and Forecast.*, **(In Press)**

Sanford, T B., J. F. Price, J. Girton, and D. C. Webb, 2007: Highly resolved observations and simulations of the oceanic response to a hurricane. *Geophys. Res. Lett.*, 34, L13604, 5 pp.

\*Shay, L.K., 2009: Upper Ocean Structure: a Revisit of the Response to Strong Forcing Events. In: *Encyclopedia of Ocean Sciences*, ed. John Steele, S.A. Thorpe, Karl Turekian and R. A. Weller, Elsevier Press International, Oxford, UK, 4619-4637, doi: 10.1016/B978-012374473-9.00628-7.

\*Shay, L. K., 2010: Air-Sea Interactions in Tropical Cyclones (Chapter 3). In *Global Perspectives of Tropical Cyclones*, 2nd Edition, Eds. Johnny C. L. Chan and J. D. Kepert, World Scientific Publishing Company: Earth System Science Publication Series, London, UK, 93-131.

Shay, L. K., A. J. Mariano, S. D. Jacob, and E. H. Ryan, 1998: Mean and near-inertial response to hurricane Gilbert. *J. Phys. Oceanogr.*, 28, 858–889.

\*Shay, L. K. and E. Uhlhorn, 2008: Loop Current Response to hurricanes Isidore and Lili, *Mon. Wea. Rev.*, 137, 3248-3274.

\*Shay, L. K., and J. Brewster, 2010: Oceanic heat content variability in the eastern Pacific Ocean for hurricane intensity forecasting. *Mon. Wea. Rev.*, **138(6)**, 2110-2131..

Taylor, K. E., 2001: Summarizing multiple aspects of model performance in a single diagram. *J. Geophys. Res.*, **106**, 7183-7192.

Teague, W. J., E. Jarosz, D. W. Wang, and D. A. Mitchell, 2007: Observed oceanic response over the upper continental slope and outer shelf during Hurricane Ivan, *J. Phys. Oceanogr.* 37, 2181-2206.

Uhlhorn, E. W., P. G. Black, J. L. Franklin, M. Goodberlet, J. Carswell and A. S. Goldstein, 2007: Hurricane surface wind measurements from an operational stepped frequency microwave radiometer. *Mon. Wea. Rev.*, 135, 3070-3085.

\*Uhlhorn, E. W., 2008: Gulf of Mexico Loop Current mechanical energy and vorticity response to a tropical cyclone. PhD Dissertation. RSMAS, University of Miami, Miami, FL 33149, 148 pp.

Walker, N., R. R. Leben, and S. Balasubramanian 2005: Hurricane forced upwelling and chlorophyll a enhancement within cold core cyclones in the Gulf of Mexico. *Geophys. Res. Letter*, 32, L18610, doi: 10.1029/2005GL023716, 1-5.